Theoret. Chim. Acta (Berl.) 53, 75–93 (1979)

THEORETICA CHIMICA ACTA

Location of Saddle Points and Minimum Energy Paths by a Constrained Simplex Optimization Procedure

Klaus Müller and Leo D. Brown

Organisch-chemisches Laboratorium der Eidg. Technischen Hochschule Zürich, Universitätsstr. 16, CH-8092 Zürich, Schweiz

Two methods are proposed, one for the location of saddle points and one for the calculation of steepest-descent paths on multidimensional surfaces. Both methods are based on a constrained simplex optimization technique that avoids the evaluation of gradients or second derivative matrices. Three chemical reactions of increasing structural complexity are studied within the PRDDO SCF approximation. Predicted properties of reaction hypersurfaces are in good overall agreement with those determined by gradient minimization and gradient-following algorithms in connection with various *ab initio* SCF methods. Computational efforts required by the new procedures are discussed.

Key words: Constrained simplex optimization method for the location of saddle points – Constrained simplex optimization method for the calculation of steepest-descent paths on multidimensional surfaces

1. Introduction

A theoretical treatment of the chemical reactivity of a molecular system requires detailed knowledge about its potential energy in terms of all internal degrees of freedom. In general, this energy function is not available analytically but can be defined numerically point by point, e.g., by several presently available quantum chemical procedures. However, the number of internal degrees of freedom grows so rapidly with increasing complexity of the molecular system that the number of evaluation points necessary for sufficient resolution may reach astronomical dimensions even for molecules of rather modest size. The task may be considerably reduced if reaction paths can be located on the potential energy hypersurface. Evaluation points may then be restricted to those spanning a grid in the domain of such paths, suitable for a dynamical treatment of chemical reactivity.

0040-5744/79/0053/0075/$03.80

There are different ways in which reaction paths can be obtained on the potential energy surface. Traditionally, some coordinate (reaction coordinate [1, 2], mapping parameter [3]) is defined along which the reaction is driven, while partial geometry optimization is performed with respect to the remaining degrees of freedom. As discussed elsewhere [2, 4, 5], reaction paths constructed in this way are by no means unique and even fail sometimes to be continuous. Alternatively, reaction paths are defined as minimum energy trajectories from saddle points to the adjoining potential energy minima, following everywhere the negative energy gradient except at the saddle point, where the initial direction is parallel to the principal axis of negative curvature [6, 7]. While this definition guarantees unique reaction paths within a given coordinate system, such minimum energy paths still depend on the coordinate system and generally do not map onto themselves under a coordinate transformation [8]. If mass-weighted Cartesian coordinates are used, gradient-following paths represent special solutions of the classical equations of motion for the nuclei [7, 9]. They define molecular relaxation processes under the conditions of infinitely slow nuclear motion and continuous dissipation of the nuclear kinetic energy. In general, this meaning is lost if minimum energy paths are calculated in other, particularly internal, coordinate systems that are not related to the mass-weighted Cartesian coordinates by an orthonormal transformation[1]. Nevertheless, the location of minimum energy paths within a given coordinate system is of considerable interest. Such paths trace the valleys on the multidimensional energy surface and are thus well suited for its exploration. They are particularly useful in detecting local intermediates lying energetically below a specified transition state. Although not uniquely defined in physical terms, they may provide rough insight into the cooperation of various internal degrees of freedom of a reacting molecular system. Finally, such paths can be used to specify the domain for additional energy evaluations required in a dynamical treatment of chemical reactivity.

By definition, minimum energy paths run between saddle points and local minima on the energy hypersurface. These points, unlike the paths between them, are uniquely defined, i.e. independently of the coordinate system. The location of energy minima on multidimensional surfaces can be performed routinely by various standard function optimization techniques [13]. By contrast, the theoretical determination of saddle points is considerably more difficult, and only a few methods have recently been advanced [4, 14–17]. One procedure consists in minimizing the Euclidean norm of the energy gradient [4, 14, 15]. This technique is quite powerful provided that the gradient is analytically available [14, 18] and that a good estimate of the saddle point region can be made in advance. However, if the gradient is calculated by finite differences the number of energy evaluations may become excessive. Furthermore, there is no guarantee that minimizing the gradient norm

---

[1] However, the physical meaning is retained if the path is defined to follow everywhere the vector $g \cdot \nabla E$, rather than the gradient ∇E itself, where g is the metric tensor, whose elements are given by $g^{ij} = \sum_k (\partial R^i/\partial \xi^k)(\partial R^j/\partial \xi^k)$ [10, 11]; R and ξ denote internal and mass-weighted Cartesian coordinates, respectively. For a special case, in which gradient-following paths remain invariant under a non-orthonormal transformation of the mass-weighted Cartesian to an internal coordinate system, see [12].

converges to a saddle point, since all local minima and maxima on the energy surface also belong to the set of possible solutions. To avoid this difficulty a modified procedure has been proposed [15], making use of the second derivative matrix of the energy. Since repeated evaluations of this matrix are required, a relatively high price is paid for the assurance of proper convergence. Finally, the specification of the domain for the search of a saddle point is often quite difficult. Chemical intuition is not always a reliable adviser. Traditional searching techniques [1, 2] require a considerable amount of energy calculations and yet may fail to locate the region for a saddle point [2, 4, 19][2]. The recently proposed "reference coordinate approach" [19], which is based on an energy contour-following algorithm, represents an interesting solution to this problem, but it requires evaluation of both the gradient and the second derivative matrix of the energy and may be too expensive for this purpose. A second procedure for the automatic location of saddle points, called the X-method [16], consists in a search for points where n linearly independent horizontal lines can be optimally fitted onto the surface of an n-parametric energy function. This method again tends to require an excessive number of energy calculations [16] and appears to have been used only once in connection with a surface of a two-parametric energy function. Finally, the "synchronous transit method" [17] has been proposed, in which the saddle point region is successively narrowed by generating linear and quadratic transit paths between limiting structures with partial geometry optimizations constrained to surfaces orthogonal to the paths. While this technique represents a promising alternative to the gradient minimization procedures, it is difficult to tell whether or not it could be used in an automatic fashion.

Once a saddle point has been located, minimum energy paths can be calculated using the gradient-following technique developed by Ishida *et al.* [9][3]. However, for each new point on the reaction path, this procedure requires evaluation of the energy gradient twice in addition to a geometry optimization orthogonal to the estimated path and thus may become rather expensive if the gradient is not analytically available.

In this paper we propose two methods, one for the location of saddle points and one for the calculation of minimum energy paths. Both methods are based on a

---

[2] A particularly instructive example is provided in [24].

[3] Alternative procedures for the calculation of minimum energy paths have been advanced in the recent literature [19–21], all of which are based on the gradient or even the second derivative matrix of the energy. Their general applicability to multidimensional surfaces appears questionable. The "reference coordinate approach" [19] may fail to produce continuous paths. The method proposed by Pancíř [20] is based on the assumption that along the valley bottom the gradient remains parallel to one of the eigenvectors of the second derivative matrix. However, this is generally not the case for steepest-descent paths [11]. Test calculations on our analytical potential (Fig. 3) revealed that paths satisfying the above criterion tend to stay on or even climb up the valley walls [22]. The method by Largo-Cabrerizo [21] attempts to calculate gradient-following paths starting in the region of an energy minimum. It is difficult to see how this can be a stable process since, near the minimum, the steepest-descent line passing through the saddle point is an asymptote to other steepest-descent lines avoiding this point [10].

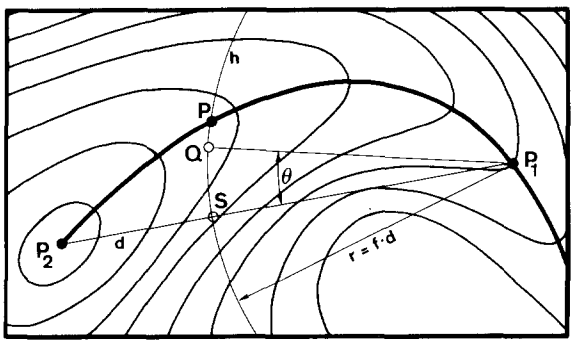

Fig. 1. Generation of an approximate path point Q between P_1 and P_2 by energy minimization on the hypersphere h with radius r starting at the point S

constrained simplex optimization technique that avoids the evaluation of gradients or second derivative matrices. The procedures are first described in context of an analytical two-parametric model potential. They are then applied to three chemical problems of increasing complexity: the isomerization of CNH to HCN, the S_N2 reaction involving H^- and CH_4, and the rearrangement of vinylidene to acetylene, the energy calculations being performed within the non-empirical PRDDO SCF MO scheme [23][4]. These reactions have been investigated by others [9, 14, 15] using gradient minimization techniques in connection with standard *ab initio* SCF MO methods and thus provide ideal testing grounds for our procedures.

2. Outline of the Basic Concept

Given two points, P_1 and P_2, on a minimum energy path, a new point, Q, lying approximately on this path may be generated between P_1 and P_2 by minimizing the energy on a hypersphere, h, centered around the higher of the two points with radius r defined as a fraction, $f < 1$, of the distance $d = |P_1P_2|$ (Fig. 1). Q will coincide with a point on the minimum energy path if the sphere intersects it at right angles. This is generally not the case for curved reaction paths. Nevertheless, Q will lie sufficiently close to the path if its curvature remains small between P_1 and P_2. Energy minimization starts at the intersection point S and is performed by means of the simplex method [25] with only the constraint that all evaluation points remain on the hypersphere h. Computational details are given in the appendix.

3. Calculation of Minimum Energy Paths

For the calculation of minimum energy paths, we identify the saddle point and an adjoining energy minimum with the starting points P_1 and P_2, respectively. The radius r can be chosen sufficiently small so that the hypersphere h intersects the

[4] Slater exponents were used for all atomic orbitals, excepting hydrogen 1s orbitals, for which exponents were set to 1.2.

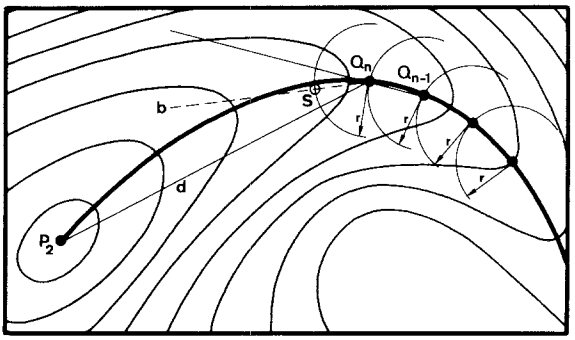

Fig. 2. Calculation of an approximate minimum energy path by generation of a series of path points Q

reaction path at approximately right angles. Energy minimization on h will then converge to a point, Q_1, essentially on the minimum energy path. Application of the same procedure to Q_1 and P_2 generates the next point on the path, Q_2, and so on. As a minor modification of the method, we take the starting point, S, for a subsequent energy minimization to be on the bisector, b, between Q_nP_2 and the extension $Q_{n-1}Q_n$ rather than on Q_nP_2 itself (Fig. 2). Generation of new points is continued until one of the following three conditions is satisfied. First, normal termination is indicated when the distance, d_n, between a point Q_n and the target point P_2 falls below a preset threshold value[5]. By then our method has produced a set of equidistant points tracing a continuous path from the saddle point to the adjoining energy minimum. This path converges to the true minimum energy path with decreasing radius r, i.e. increasing number of path points. Second, the procedure is halted when a new point on the path is energetically higher than a previous one, indicating passage through a local intermediate. Unconstrained energy minimization is then performed to locate the proper position of this intermediate. Third, calculations are stopped if no energy minimum is found on the frontal hemisphere of h[6], indicating movement away from the target point P_2. This situation may occur if P_2 does not represent an energy minimum adjoining the saddle point under investigation.

To illustrate the procedure we apply it to the surface of a two-parametric model potential[7] having three minima and two saddle points. Maps of equipotential curves are shown in Fig. 3. Since the gradient is analytically available, accurate minimum energy paths can be calculated without difficulties. They are indicated

---

[5] A threshold value of $1.2r$ has proved satisfactory.

[6] The frontal hemisphere includes all points on h for which the azimuthal angle, θ, with respect to the axis P_1S (Fig. 1) or Q_nS (Fig. 2) does not exceed $\pi/2$.

[7] The potential consists in a sum of four terms of the form $A \cdot \exp[a(x - x_0)^2 + b(x - x_0)(y - y_0) + c(y - y_0)^2]$, in which the constants take the following values: (A) = (−200/−100/−170/15), (a) = (−1/−1/−6.5/0.7), (b) = (0/0/11/0.6), (c) = (−10/−10/−6.5/0.7), (x_0) = (1/0/−0.5/−1), (y_0) = (0/0.5/1.5/1).

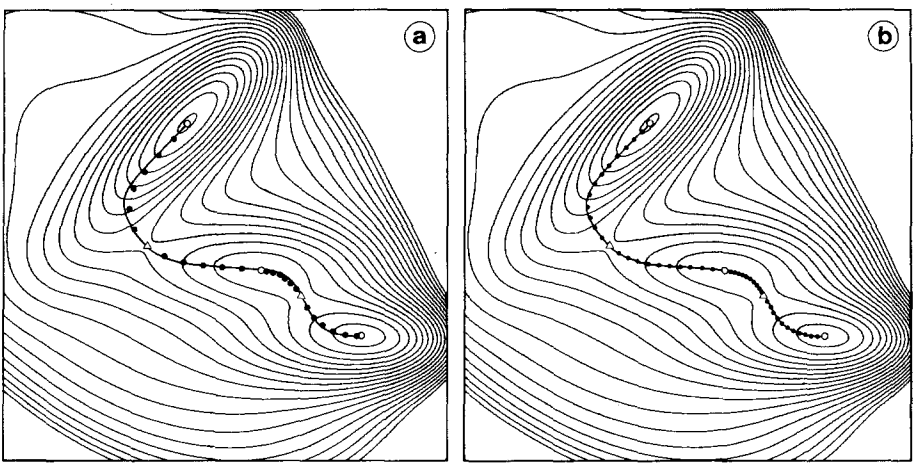

Fig. 3a and b. Series of path points (solid circles) generated in the calculation of minimum energy paths on the two-parametric model potential[7] using $f = 1/6$ (case **a**) and $f = 1/11$ (case **b**). Each series starts at a saddle point (triangle) and ends at an energy minimum (open circle)

by the solid lines connecting minima with saddle points. Figures 3a and 3b show the results of our procedure when the radius r is set equal to, respectively, 1/6 and 1/11 of the distance between a saddle point and an adjoining minimum. Deviations of the calculated points from the true minimum energy paths are evident in Fig. 3a. They are most pronounced in the upper section of the contour map, where the reaction path is strongly curved. These deviations are quite systematic. In general, our procedure tends to underestimate the curvatures of gradient-following paths. On the other hand, an approximate doubling of the number of path points is sufficient to reduce these deviations to the extent that, for practical purposes, the set of points can be regarded as a good approximation to the true minimum energy paths (Fig. 3b).

4. The Location of Saddle Points

To locate a saddle point between two energy minima, we generate valley points of increasing energy, closing in on the saddle point from opposite sides. Valley points are obtained by means of the general procedure outlined in Sect. 2 (Fig. 1), starting with the two energy minima as P_1 and P_2. A fixed value of $f > 0.5$ is used for the ratio of radius r to distance d so that the hypersphere h is most likely to encompass the saddle point region. Empirically, a ratio of $f = 2/3$ has proved satisfactory. Each time a valley point is generated, an energy/distance analysis is carried out to select a new (P_1, P_2) pair which is used in the search for the next valley point. The three typical situations which can occur in this analysis are schematically depicted in Fig. 4. P_1' and P_2' denote the two points between which the valley point Q was generated on the preceding cycle. The (P_1, P_2) pair for the next cycle is then determined as follows. If Q is of higher energy than both P_1' and P_2' (Fig. 4a), Q is taken

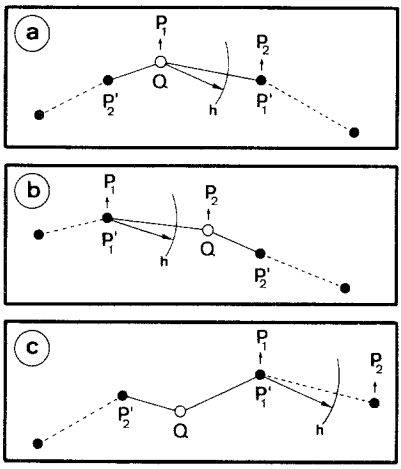

Fig. 4a–c. The three typical situations encountered in the energy/distance analysis of the saddle point location procedure

as P_1 and the more distant of its two neighboring points is used as P_2. If Q lies energetically between P_1' and P_2' (Fig. 4b), or if Q is below both P_1' and P_2' (Fig. 4c), the highest of the three points is selected as P_1 with its more distant neighboring point as P_2. The occurrence of a situation of the third kind (Fig. 4c) is taken as an indication for the existence of a local intermediate between the two original energy minima. While the search for one saddle point is continued, the low-lying valley point is flagged so that the surface around it can be explored at a later stage by unconstrained energy minimization. Valley points generated during the initial phase of the location process may deviate substantially from minimum energy paths because the searching radii are quite large at the beginning and reaction paths are rarely straight. However, in the course of closing in on the saddle point, the radii become progressively smaller and new valley points fall more and more closely on both minimum energy paths. Eventually, a situation of the first kind (Fig. 4a) is encountered in which the searching radius gets smaller than a preset threshold value, $r_{\min}$. The saddle point is then sufficiently narrowed down so that it can be located simply by finding the highest point along the straight paths from P_1' to Q and from Q to P_2'. To verify its saddle point nature, an energy minimization is performed in the subspace orthogonal to the straight path through the highest-energy point. The test is considered successful if this geometry optimization converges to the same structure within prespecified numerical accuracy.

As an illustration we apply the procedure to the surface of the analytical, two-parametric model potential of the previous section[7]. The parameters and energies of the two saddle points, as determined by minimizing the norm of the energy gradient, are given in Table 1. There are three minima on this surface, hence six possible ways in which the procedure can be applied, depending on the choice of the initial (P_1, P_2) pair. In each case one of the two saddle points is correctly located within a desired numerical accuracy of about ± 0.01 for each parameter[8] (Table 1).

---

[8] Calculations were performed with $s_{\text{conv}} = 0.01$ (see appendix) and $r_{\min} = 0.04$.

Table 1. Energy minima and saddle points of the analytical, two-parametric model potential[7]

		Energy minima[a]						
		E	x	y				
Minimum A		−146.700	−0.558	1.442				
Minimum B		−108.167	0.623	0.028				
Minimum C		−80.768	−0.050	0.467				
		Saddle points[b]						
		E	x	y	E	x	y	
		−40.665	−0.822	0.624	−72.249	0.212	0.293	
		Saddle points[c]						
Run	(P_1, P_2)	E	x	y	E	x	y	N[d]
1	(A, B)	−40.67	−0.82	0.62	—			124
2	(B, A)	−40.68	−0.82	0.62	—			155
3	(B, C)	—			−72.26	0.22	0.29	74
4	(C, B)	—			−72.27	0.21	0.30	73
5	(A, C)	−40.68	−0.81	0.62	—			112
6	(C, A)	−40.67	−0.82	0.62	—			113

[a] Determined by unconstrained energy minimization using the simplex method [25].
[b] Determined by minimization of $|\nabla E|^2$.
[c] Determined by the constrained simplex optimization procedure[8].
[d] Total number of function evaluations.

Valley points generated in run 1 of Table 1 are displayed in the contour diagram of Fig. 5.

The following features are typical for the performance of the procedure. Valley points generated early may deviate substantially from minimum energy paths. Nevertheless, they already provide a rough insight into the course of the reaction paths. At a later stage they represent better path points, approaching the saddle point from opposite sides. Only one of the two saddle points is located in this run. However, valley point 4 is properly diagnosed to fall into the region of a local intermediate, the position of which is determined by unconstrained energy minimization starting around this point. The second saddle point is then obtained by reapplication of the location procedure using this local intermediate either as P_1 or P_2 (runs 4 and 3 of Table 1, respectively).

For proper performance of the location procedure, we must ensure that, in each cycle, a new valley point Q (Fig. 1) is located in the region between the points P_1 and P_2 and not behind P_1. However, under certain circumstances there is no energy minimum on the frontal hemisphere of h[6] so that an unlimited search for it would inevitably converge to an undesired valley point on the backside of P_1. Figure 6 shows

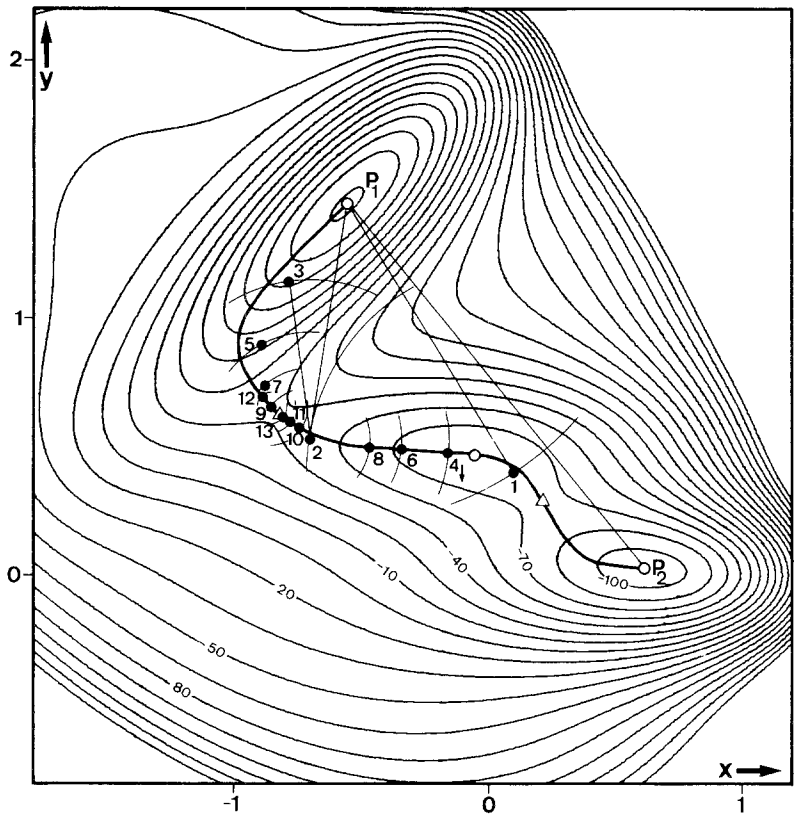

Fig. 5. The series of valley points generated in run 1 of Table 1 for the location of a saddle point on the two-parametric model potential[7]

two typical situations where this problem may be encountered. In the first case (Fig. 6a) an early generated point, which happens to fall into the saddle point region but not very close to the reaction path, is used as P_1 at a later stage, when the searching radius is small. Energy minimization on h may then fall right through the saddle point. In fact, this occurred once during the location of a saddle point on the two-parametric model potential (Table 1, run 2). A simple remedy procedure proved quite effective in coping with situations of this type. It consists of finding the valley point Q by energy minimization in the subspace orthogonal to P_1P_2 through the midpoint MP (Fig. 6a). Both P_1 and P_2 are then eliminated from the list of valley points, and the location procedure is resumed at the energy/distance analysis for Q and its two neighboring points taken as P_1' and P_2' according to Figs. 6a and 4a. In the second case (Fig. 6b) the location procedure is applied to two energy minima, between which there is no saddle point but only a ridge separating two divergent reaction valleys. Such a situation may occur on complicated multi-minima potential surfaces [26]. In the case at hand a short series of apparent valley points first simulates the existence of a saddle point. At a certain stage, however, suitable valley

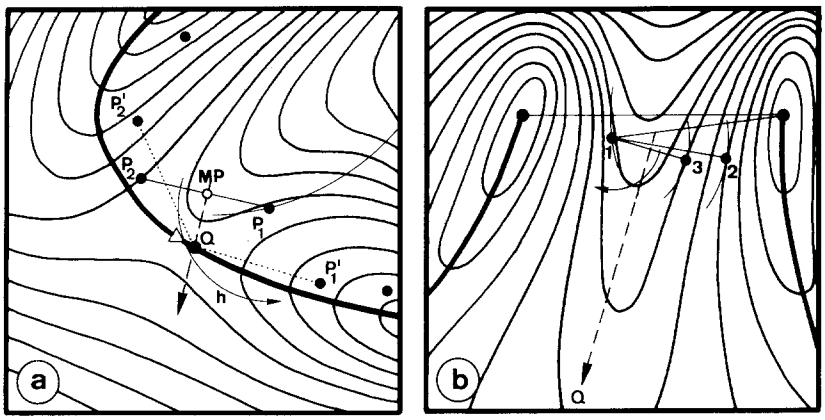

Fig. 6a and b. Two typical situations where energy minimization on a hypersphere fails to locate a valley point in the region between P_1 and P_2. The performance of the remedy procedure is shown schematically

points can no longer be located. Use of the remedy procedure results in a long journey down the ridge to a point Q far removed from the region of the initial search. This point may be of value for further explorations of the potential surface, e.g., by application of the location procedure to Q as one of two starting points or by means of unconstrained energy minimization around Q.

5. The Isomerization of CNH to HCN

This reaction is of considerable chemical and theoretical interest and has been investigated by *ab initio* SCF calculations at various basis set levels [8, 9, 14]. It involves three degrees of freedom but is of sufficient structural complexity to serve as a test case for our procedures. Furthermore, the saddle point and minimum energy paths have been determined by gradient minimization [14] and gradient-following [9] algorithms, respectively, thus providing a valuable basis for comparison[9].

Two distances, r(CN) and r(CH), and one angle, γ(HCN), are chosen as independent parameters. Unconstrained energy minimization for the two isomers leads to the structural parameters shown in Table 2. They are in acceptable agreement with, if systematically larger than, bond lengths obtained from accurate *ab initio* SCF methods. The predicted exothermicity of the isomerization reaction is well within the range of previous theoretical estimates. The location procedure may be applied in two different ways, depending on the choice of the starting points P_1 and P_2. In either case one and the same saddle point is located within numerical errors of less than ± 0.005 Å and $\pm 0.5°$. Its structure and relative energy agree well with the

[9] PRDDO has been shown [23, 27] to reproduce closely the results of accurate *ab initio* SCF calculations using minimum basis sets.

Table 2. Properties of the CNH—HCN potential energy surface, predicted within the PRDDO approximation and by various *ab initio* SCF methods[a].

		PRDDO	STO-3G [14]	4-31G [14]	DZ-P[b] [8]	DZ-P/CI[b] [8]
HCN[c]	r(CN)	1.176	1.15	1.14	1.137	1.150
	r(CH)	1.093	1.07	1.05	1.062	1.066
	E_{rel}	0	0	0	0	0
CNH	r(CN)	1.184	1.17	1.16	1.159	1.170
	r(NH)	1.020	1.01	0.98	0.986	0.996
	E_{rel}	10.1	19.3	9.5	9.5	14.6
saddle point	r(CN)	1.23	1.22	1.18	1.174	1.181
	r(CH)	1.26	1.20	1.21	1.153	1.171
	γ(HCN)	71.2	73.0	71.1	78.8	74.9
	E_{rel}	62.9	69.2	67.1	49.7	49.5

[a] Distances in Å, angles in degrees, relative energies in kcal/mole.
[b] Results calculated from the data given in [8].
[c] Experimental values are r(CN) = 1.153 Å and r(CH) = 1.065 Å [28].

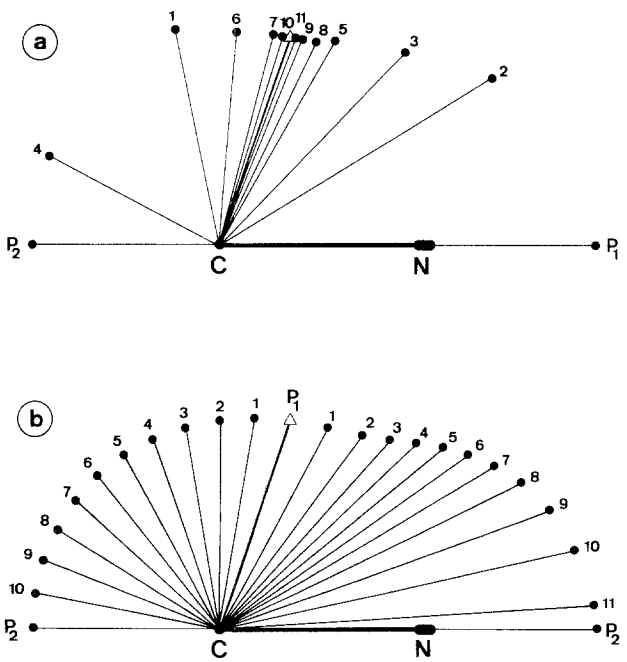

Fig. 7a. Valley points generated for the location of the saddle point (open triangle) on the CNH–HCN potential energy surface. **b** Complete isomerization path, traced by two sets of points obtained by application of the minimum energy path procedure to the saddle point (P_1) and each of the two energy minima (P_2) using $f = 1/11$

results given in [14]. Valley points generated in the location run using CNH as starting point P_1 are shown in Fig. 7a. These points alone may suffice to characterize major portions of the isomerization path. The complete path is accurately traced by the two sets of points produced by the minimum energy path procedure when applied to the saddle point and each of the two isomers with $f = 1/11$ (Fig. 7b). For infinitely slow motion the hydrogen atom starts and terminates on essentially circular paths centered around the nitrogen and the carbon atom, respectively, but, in between, proceeds more or less parallel to the CN bond. The isomerization is accompanied by a slight transitory lengthening of the CN bond, being most pronounced when the hydrogen atom moves alongside. Our predictions are in full harmony with previous results [8, 9].

6. The S_N2 Reaction Involving H^- and CH_4

The saddle point of this reaction has invariably been shown to have a trigonal bypyramidal structure [9, 29–32]. The steepest-descent path leading from there to separated CH_4 and H^- has been calculated within the STO-3G minimum basis set approximation [9] and found to differ substantially from a reaction path obtained at a higher basis set level [30] but using one C—H distance as an arbitrary reaction coordinate. Assuming conservation of three-fold symmetry, the potential energy function is given in terms of four independent parameters, e.g. three CH distances and one HCH angle (Fig. 8). Starting with two symmetry-related configurations, structurally optimized with one CH distance maintained at 2.7 Å (P_1 and P_2 in Fig. 8a), a saddle point of D_{3h} symmetry is successfully located after generation of twelve valley points. The predicted CH bond lengths of 1.54 Å and 1.10 Å for the axial and equatorial hydrogen atoms, respectively, are identical with those obtained by minimizing the energy of CH_5^- under the constraint of D_{3h} symmetry[10]. The series of valley points provides a rough picture of the S_N2 reaction path, which is accurately traced by the two symmetry-related sets of points produced by the minimum energy path procedure with $f = 1/11$ (Fig. 8b). Our path is in qualitative agreement with that following the negative gradient on the STO-3G potential energy surface [9].

7. The Rearrangement of Vinylidene to Acetylene

This reaction was examined by Poppinger [15] as a test case for a saddle point location procedure based on an improved gradient minimization technique. Calculations were performed at the STO-2G level for an in-plane rearrangement. The same reaction has recently been studied at a double-ζ and extended basis set level both with and without inclusion of electron correlation [37]. The overall agreement of our results with the various theoretical predictions (Table 3) is satis-

[10] These values are well within the ranges of 1.48–1.75 Å and 1.06–1.13 Å for $r(CH_{ax})$ and $r(CH_{eq})$, respectively, as calculated by *ab initio* SCF methods at various basis set levels [9, 29–36].

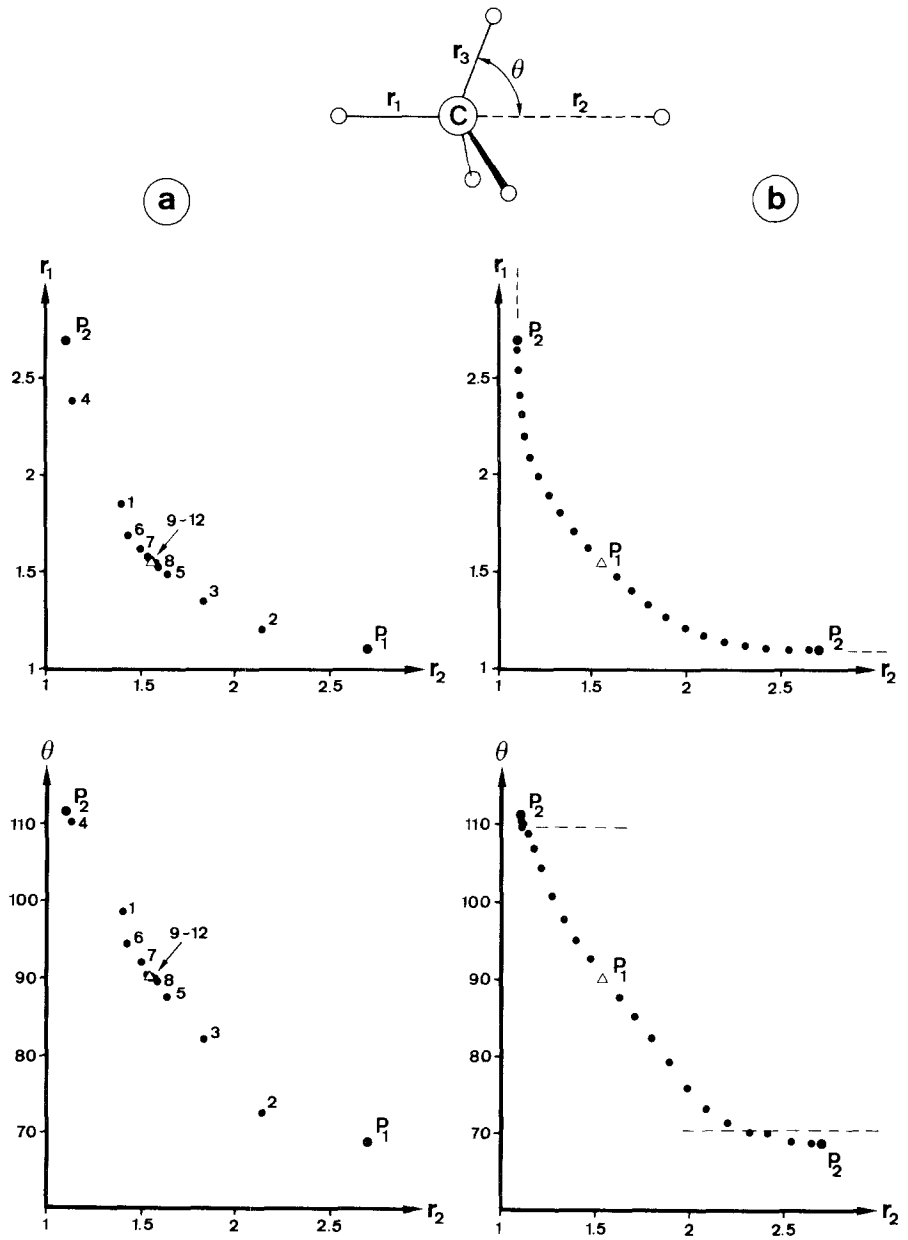

Fig. 8a. Valley points generated for the location of the saddle point (open triangle) on the $H^- + CH_4$ S_N2 potential energy surface

b S_N2 reaction path traced by the two sets of points obtained by application of the minimum energy path procedure to the saddle point (P_1) and one of the two symmetry-related limiting configurations P_2 using $f = 1/11$. Dashed lines indicate parameter values for $r_2 = \infty$. Distances are in Å, angles in degrees

Table 3. Properties of the $H_2C{=}C{-}HC{\equiv}CH$ potential energy surface, predicted within the PRDDO approximation and various *ab initio* SCF methods with partial inclusion of electron correlation[a]

		STO-2G [15]	DZ/SCEP [37]	PRDDO
$HC{\equiv}CH$ ($D_{\infty h}$)[b]	r(CC)	1.178	1.230	1.204
	r(CH)	1.075	1.071	1.086
	E_{rel}	0	0	0
$H_2C{=}C$ (C_{2v})	r(CC)	1.316	1.342	1.323
	r(CH)	1.086	1.096	1.096
	γ(CCH)	121.4	121.1	121.8
	E_{rel}	40.8	45.7 (40.0)[d]	24.3
saddle point (C_s)[c]	r(CC)	1.264	1.289	1.28
	r(CH_1)	1.437	1.418	1.48
	r(CH_2)	1.084	1.079	1.09
	γ(CCH_1)	52.8	55.2	54.6
	γ(CCH_2)	178.2	176.1	174.7
	E_{rel}	72.6	63.6 (48.6)[d]	66.8

[a] Distances in Å, angles in degrees, relative energies in kcal/mole.
[b] Experimental values are r(CC) = 1.203 Å, r(CH) = 1.061 Å [28].
[c] Structural parameters according to Fig. 9.
[d] Energies in parentheses from extended basis set calculations with inclusion of electron correlation (DZ-P/SCEP) for selected points on the DZ/SCEP potential energy surface [37]. An exothermicity of 46 kcal/mole has been estimated based on generalized valence bond configuration interaction calculations [38].

factory. There are six degrees of freedom, but only five structural parameters are required if C_s symmetry is imposed. They are chosen as shown in Fig. 9. Application of the location procedure using either vinylidene or acetylene as starting point P_1 leads to one and the same saddle point within numerical errors of less than ± 0.005 Å and $\pm 0.5°$[8]. This same saddle point is located without any symmetry assumption, i.e., with inclusion of an out-of-plane angle, τ(HCCH), as the sixth independent parameter. Since both the saddle point and the two equilibrium configurations are planar, the rearrangement must take place within the common symmetry plane according to group theoretical arguments [39]. Indeed, the same set of valley points (Fig. 9a) is generated by the location procedure, whether or not C_s symmetry is imposed. As noted in previous sections, these points alone provide a qualitatively correct picture of the reaction path (Fig. 9b), which is obtained by application of the minimum energy path procedure to the saddle point and each of the two C_2H_2 isomers using $f = 1/11$.

The path traced by the hydrogen atom, H_1, moving around the CC unit, is strikingly similar to that found in the isomerization of CNH to HCN (Fig. 7b). The other hydrogen atom, H_2, performs an oscillation as indicated by the arrow in Fig. 9b.

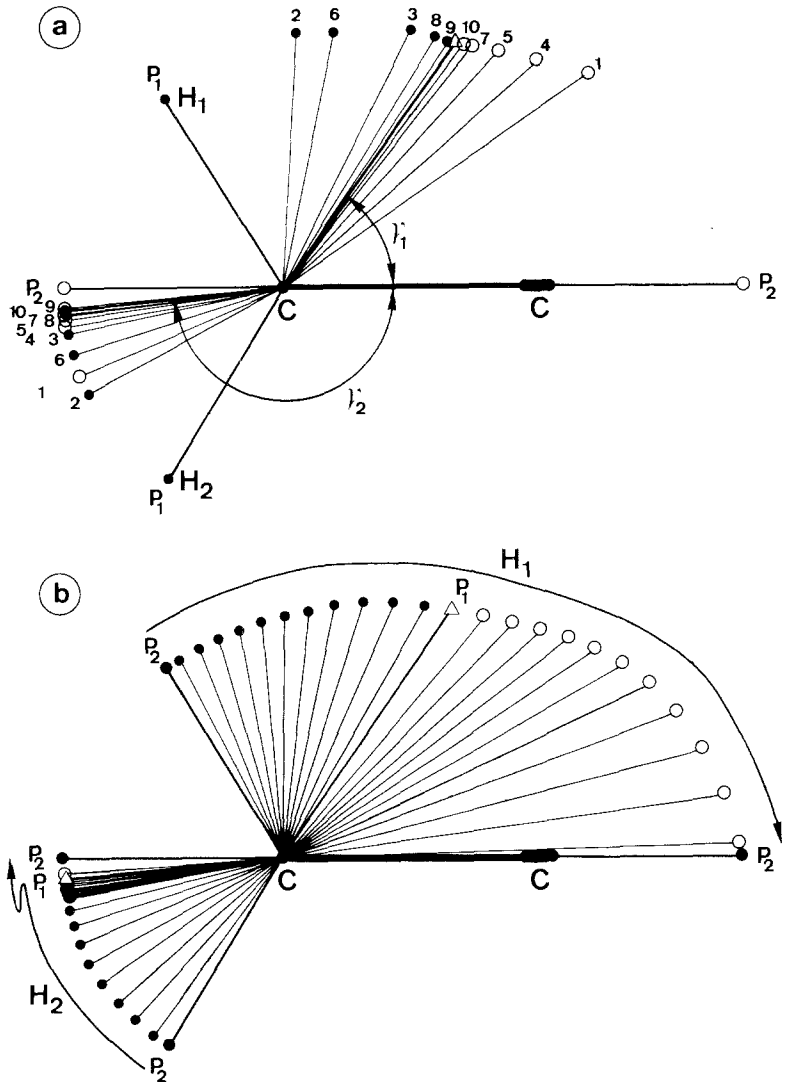

Fig. 9. a Valley points generated for the location of the saddle point (open triangle) on the $H_2C{=}C{-}HC{\equiv}CH$ potential energy surface. **b** Complete rearrangement path, traced by two sets of points obtained by application of the minimum energy path procedure to the saddle point (P_1) and each of the two equilibrium configurations (P_2) using $f = 1/11$

Our results suggest that the rearrangement starts out along the antisymmetric in-plane bending coordinate of vinylidene. After passage through the saddle point, the hydrogen atom H_2 swings back while H_1 continues to move ahead so that the reaction path terminates along an asymptote to the centrosymmetric bending of acetylene.

8. The Computational Effort

Having demonstrated the successful performance of the new procedures, a few comments are in place concerning their efficiency. Of course, any generalization should be taken with care since the complexity of a potential energy surface may vary dramatically from one reaction to the other. Moreover, the total number of energy evaluations depends not only on the desired numerical accuracy but also on the starting conditions for the location of a saddle point and on the density of path points for the description of a minimum energy path. To ease comparison all saddle points were determined to the same level of accuracy, 0.005 Å for distances and 0.5° for angles[8], always starting from two equilibrium structures or, as in the S_N2 reaction, from two sufficiently distant limiting configurations. Likewise, minimum energy paths were determined uniformly by sets of at least ten path points ($f = 1/11$), calculated within numerical errors of less than 0.002 Å and 0.2° for distances and angles, respectively. With these prerequisites an empirical relationship between N, the total number of energy calculations needed for the location of a saddle point, and n, the number of internal degrees of freedom, is found (Fig. 10), which is approximately given by

$$N = 11.5n(n + 3).$$

Essentially the same relationship is also obtained for the total number of evaluation points used in calculating a minimum energy path. Evaluation of the gradient and the second derivative matrix of the energy by finite differences requires a minimum of, respectively, $(n + 1)$ and $0.5(n + 1)(n + 2)$ energy calculations. Hence, assuming that gradients are not analytically available, the computational effort involved in obtaining a saddle point or a minimum energy path by one of the new procedures

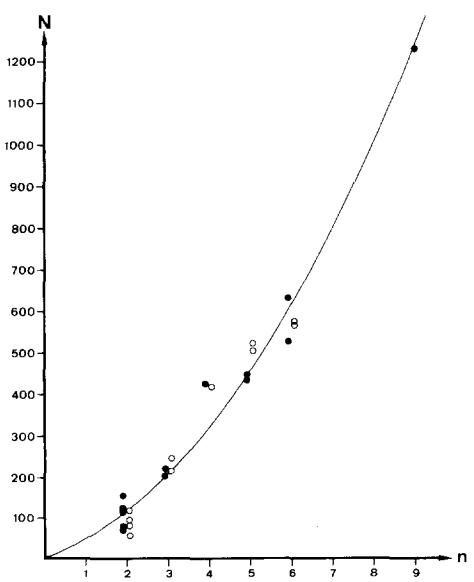

Fig. 10. Total number of energy evaluations, N, required for the location of a saddle point (solid circles) and for the calculation of a minimum energy path (open circles), plotted against n, the number of internal degrees of freedom. The relationship $N = 11.5\ n\ (n + 3)$ is shown by the solid line. Also included is N for $n = 9$, obtained in a preliminary study of the H_3NO—H_2NOH potential energy surface [22]

is roughly equivalent to $11.5(n + 2)$ calculations of the gradient or 23 evaluations of the second derivative matrix. For minimum energy paths this effort appears to be comparable to that of the gradient-following algorithm of Ishida *et al.* [9], at least for surfaces of moderate dimensionality. The effort required by the saddle point location procedure seems to be somewhat excessive at first sight. However, this is due to the fact that location is started at two equilibrium configurations. If a good estimate of the saddle point region can be made in advance, two more closely lying configurations may be used as starting points P_1 and P_2. In this way the number of evaluation points is dramatically reduced. On the other hand, starting from energy minima has definite advantages: it allows us to locate saddle points in a chemically unbiased way, requiring knowledge only about equilibrium structures. At the same time, it provides us with a set of valley points which, in many cases, may be quite adequate for a qualitative description of reaction paths.

Appendix

Computational details are given for the constrained simplex optimization procedure.

The independent structural parameters R_i ($i = 1, 2, \ldots, n$), specifying a molecular system, are taken to span a Euclidean n-space. The dimensions for bond distances and angles are Bohrs (=0.529 Å) and radians, respectively. This choice provides a scaling which has proved advantageous in geometry optimizations. The method for constrained energy minimization is outlined with reference to Fig. 1. A regular $(n - 1)$-dimensional simplex is set up by an $n \times n$ matrix P'', the rows of which hold the vector components for each of the points P_k'' ($k = 1, 2, \ldots, n$). P'' is given by

$$P'' = T \cdot U + v. \tag{1}$$

The transformation matrix U, obtained by the method of Powell [40], defines a Cartesian coordinate system with one axis parallel to P_1P_2. The matrix T generates a regular $(n - 1)$-dimensional simplex within the subspace orthogonal to this distinguished axis. The row vector v shifts the simplex centroid from the origin to point S. Projection of all points P_k'' onto the hypersphere h according to (2) yields the set of points P_k'.

$$\begin{aligned} P_k' &= x \cdot P_k'' + (1 - x) \cdot P_1 \quad \text{for} \quad k = 1, 2, \ldots, n \\ x &= |P_1S|/|P_1P_k''| \end{aligned} \tag{2}$$

They define the starting simplex for the constrained optimization procedure, which differs from the original simplex algorithm [25] only by the fact that any newly generated point is projected onto h according to (2) prior to an energy evaluation.

Let the size of a simplex be defined by s, the rms distance between the centroid P_c and the corner points P_k' (3),

$$s = \left(\sum_k |P_k'P_c|^2/n \right)^{1/2}. \tag{3}$$

Convergence is indicated when s falls below a preset threshold value s_{conv}. Determination of the approximate minimum energy position then includes both the centroid and the corner points. Values of 0.01 and 0.003 have been used for s_{conv} in saddle point locations and minimum energy path calculations, respectively. The number of evaluation points needed for convergence depends critically on the size, s_0, of the starting simplex. Numerical experience has shown $s_0 = 1/5|P_1S|$ to be quite appropriate in both types of calculations.

Acknowledgement. This work was partly supported by Hoffmann-La Roche & Co., Basle. One of us (L.D.B.) wishes to thank the Swiss National Science Foundation for a postdoctoral fellowship. A generous grant of computing time by the ETHZ computing center is gratefully acknowledged.

References

1. Empedocles, P.: Intern. J. Quantum Chem. **3S**, 47 (1969)
2. Dewar, M. J. S., Kirschner, S.: J. Am. Chem. Soc. **93**, 4290, 4291, 4292 (1971)
3. Ermer, O.: Struct. Bonding (Berlin) **27**, 161, 202 (1976)
4. McIver, Jr., J. W., Komornicki, A.: J. Am. Chem. Soc. **94**, 2625 (1972)
5. Komornicki, A., McIver, Jr., J. W.: J. Am. Chem. Soc. **96**, 5798 (1974)
6. Fukui, K.: J. Phys. Chem. **74**, 4161 (1970)
7. Fukui, K., Kato, S., Fujimoto, H.: J. Am. Chem. Soc. **97**, 1 (1975)
8. Pearson, P. K., Schaefer III, H. F., Wahlgren, U.: J. Chem. Phys. **62**, 350 (1975)
9. Ishida, K., Morokuma, K., Komornicki, A.: J. Chem. Phys. **66**, 2153 (1977)
10. Basilevsky, M. V.: Chem. Phys. **24**, 81 (1977)
11. Tachibana, A., Fukui, K.: Theoret. Chim. Acta (Berl.) **49**, 321 (1978)
12. Murrell, J. N.: Struct. Bonding (Berl.) **32**, 93, 100 (1977)
13. Dixon, L. C. W.: Nonlinear optimization. London: The English Universities Press Limited, 1972
14. Komornicki, A., Ishida, K., Morokuma, K., Ditchfield, R., Conrad, M.: Chem. Phys. Letters **45**, 595 (1977)
15. Poppinger, D.: Chem. Phys. Letters **35**, 550 (1975)
16. Mezey, P. G., Peterson, M. R., Csizmadia, I. G.: Can. J. Chem. **55**, 2941 (1977); Peterson, M. R., Csizmadia, I. G., in: Applications of MO theory in organic chemistry, I. G. Csizmadia, Ed., Vol. 2, p. 117. Amsterdam: Elsevier Scientific Publishing Company, 1977
17. Halgren, T. A., Lipscomb, W. N.: Chem. Phys. Letters **49**, 225 (1977)
18. Fletcher, R.: Mol. Phys. **19**, 55 (1970); Dupuis, M., King, H. F.: J. Chem. Phys. **68**, 3998 (1978)
19. Nalewajski, R. F., Carlton, T. S.: Acta Phys. Pol. **A53**, 321 (1978)
20. Pancíř, J.: Collect. Czech. Chem. Commun. **40**, 1112 (1975)
21. Largo-Cabrerizo, J.: An. Quim. **73**, 1092 (1977)
22. Müller, K.: unpublished results
23. Halgren, T. A., Lipscomb, W. N.: J. Chem. Phys. **58**, 1569 (1973)
24. Jug, K.: Theoret. Chim. Acta (Berl.) **42**, 303 (1976)
25. Nelder, J. A., Mead, R.: Comput. J. **7**, 308 (1964/5)
26. Müller, K., Brown, L. D.: to be published
27. Halgren, T. A., Kleier, D. A., Hall, Jr., J. H., Brown, L. D., Lipscomb, W. N.: J. Am. Chem. Soc. **100**, 6595 (1978)
28. Landolt-Börnstein: Numerical data and functional relationships in science and technology, New Series, Vol. II/7. Berlin: Springer-Verlag, 1976
29. Ritchie, C. D., Chappell, G. A.: J. Am. Chem. Soc. **92**, 1819 (1970)

30. Dedieu, A., Veillard, A.: J. Am. Chem. Soc. **94**, 6730 (1972)
31. Baybutt, P.: Mol. Phys. **29**, 389 (1975)
32. Leforestier, C.: J. Chem. Phys. **68**, 4406 (1978)
33. Van der Lugt, W. Th. A. M., Ros, P.: Chem. Phys. Letters **4**, 389 (1969)
34. Mulder, J. J. C., Wright, J. S.: Chem. Phys. Letters **5**, 445 (1970)
35. Dyczmons, V., Kutzelnigg, W.: Theoret. Chim. Acta (Berl.) **33**, 239 (1974)
36. Keil, F., Ahlrichs, R.: J. Am. Chem. Soc. **98**, 4787 (1976)
37. Dykstra, C. E., Schaefer III, H. F.: J. Am. Chem. Soc. **100**, 1378 (1978)
38. Davis, J. H., Goddard III, W. A., Harding, L. B.: J. Am. Chem. Soc. **99**, 2919 (1977)
39. Stanton, R. E., McIver, Jr., J. W.: J. Am. Chem. Soc. **97**, 3632 (1975)
40. Powell, M. J. D.: Comput. J. **11**, 302 (1968)

Received February 23, 1979/May 14, 1979